A Time Scenes Simulation Using Multiple Regression of the Discrete Cosine Transform of Color Block's Time Images

作者 1：
Chen-Chung Liu
Chin-Yi Institute of Technology
Electronic Engineering Depart.
Lecturer
ccl@ncit.edu.tw

作者 **2**：
Kai-Wen Chuang
Chin-Yi Institute of Technology
Electronic Engineering Depart.
Student
n0703124@yahoo.com.tw

作者 3：
Wen-Yuan Chen
Chin-Yi Institute of Technology
Electronic Engineering Depart.
Associate Professor
cwy@ncit.edu.tw

作者 4：
Chi-Chao Yang
Chin-Yi Institute of Technology
Electronic Engineering Depart.
Student
guitar3931@yahoo.com.tw

中文摘要

本文介紹一個針對室外風景影像在任何時間的模擬影像之高效率、新穎的演算法。此演算法結合了離散餘弦變換、表格查尋及統計的多元回歸。首先，我們使用在同一天的固定時間間距的顏色方塊之影像，將它們作離散餘弦轉換(Discrete Cosine Transform)後作為室外風景影像之時間模擬的參考數據庫。然後， 我們從這個參考數據庫建立光的三原色(紅色、綠色、藍色)隨時間變化之多元回歸最佳貼合函數(best fitting functions)。最後，使用輸入風景影像和原始時間之時間模擬影像演算法(TSSA)於焉完成。

為展示我們提出的演算法的效率，我們輸入且模擬各種各樣的室外風景影像。實驗結果證明，我們提出的演算法可以從輸入的室外風景影像精確地模擬出該室外風景影像在任何時間的模擬影像。

關鍵詞： 離散餘弦變換、表格查尋、 多元回歸、 模擬.

Abstract

In this paper, an efficient novel strategy simulating time scenes of an outdoor scene is introduced. It is a hybrid approach combining the multiple regression in statistic, the discrete cosine transform, and a look-up table algorithm. First, several color-block images taken at different times of a day were used as the testing images to create the reference database of the time scene. We then establish best fitting functions of light intensity in each plane (red, green, blue) with respect to time individually. These best fitting functions were generated by taking the multiple regressions on those coefficients of the DCT blocks of the color-block images. Finally, the time scenes simulation algorithm (TSSA) is able to synthesize the simulation scene at any assigned time by using the original input image.

To explore the utility and demonstrate the efficiency of the proposed algorithm, simulations under various input images are conducted. The experiment results show that our proposed algorithm can precisely simulate the desired scenes at an assigned time and has three advantages: (A) Using the color-block images instead of using the scene images of a place to create the reference database, the database can be used for any outdoor scene taken at anywhere at anytime. (B) Taking the multiple regression on the DCT coefficients of scene images instead of taking the multiple regression on the spatial pixels of scene images, it simplifies the regression procedure and save the processing time. (C) Using look-up table algorithm to save time.

Keywords: Discrete Cosine Transform, Look- up Table, Multiple Regressions, Simulation.

1. Introduction

Sunrise and Sunset are the most beautiful scenes of a day, but they appear only in a very short time interval and people are almost always too busy to wait for their coming. If one can construct the sunset (or sunrise) scene of a scene image taken at anytime, then people shall no longer regret of missing the beautiful moments of their life.

The most special difference between a noon scene and a dusk (or dawn) scene is the colors of the sun and the sky. The Earth's atmosphere contains both air molecules and tiny aerosols (much tinier than the wavelength of the visible light-ray from the Sun), both of which scatter the visible light-ray from the Sun which grazes the Earth's atmosphere; Figure 1 shows the phenomena (scattering, reflection, transmitting and absorption) of a sunlight's beam striking a partially transparent material (the Earth's atmosphere).

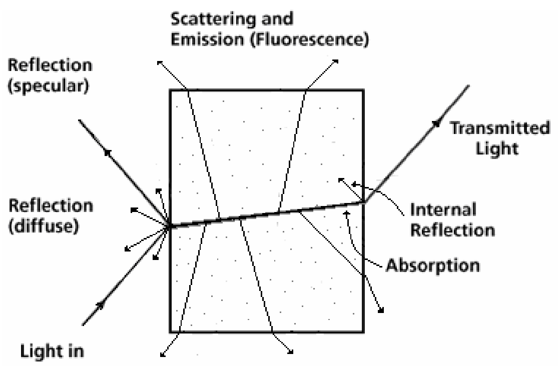

Figure 1. the phenomena of a sunlight's beam striking a partially transparent material block. (Taken from " The Physics and Chemistry of Color ". Kurt Nassau (John Wiley & Sons, New York, 1983).)

The scattering from both air molecules and aerosols is predominantly the Rayleigh scattering [1- 4].The intensity I of light scattered by a single tiny particle from a beam of light is given by

$$I = I_0 \frac{(1+\cos^2\Phi)}{2R^2}\left(\frac{2\pi}{\lambda}\right)^4\left(\frac{n^2-1}{n^2+2}\right)^2\left(\frac{d}{2}\right)^6 \qquad (1)$$

where I_0 is the original intensity of entrance light, Φ is the scattering angle between the direction of incidence and the direction of observation., R is the large distance from the particle to the observer, λ is the wavelength of entrance light, n is the refractive index of particle, and d is the diameter of the particle. The Rayleigh scattering coefficient for a group of scattering particles is the multiplication product of the concentration of particles N and the cross-section σ_s.

$$\sigma_s = \frac{2\pi^5}{3}\frac{d^6}{\lambda^4}\left(\frac{n^2-1}{n^2+2}\right)^2 \qquad (2)$$

According to the Rayleigh scattering law of light, the scattered light is polarized at a large angle with respect to the direction of the sun's light and blue light is scattered more strongly than red light. When the sun high in the sky, sunlight goes through very little atmosphere, so little scattering takes place, the sky far away to the sun appears light blue and the sky close to the sun appears mostly white (the sun's color). When the Sun is low in the sky at sunrise or at sunset, the Sun's light has to travel through a much thicker layer of atmosphere to reach us on the ground owing to the oblique angle as shown in Fig. 2.

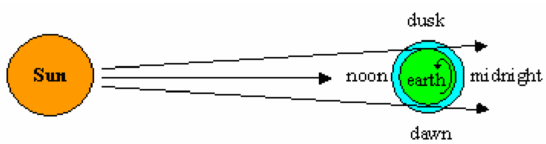

Fig.2 the oblique angle and the path of sunlight at different time

This extra distance causes multiple scatterings of blue light, The sky appears less bright and redder than that at noon because more blue light than red light is scattered out of the solar light-rays, leaving an excess of red light.

It is very difficult to obtain the concentration and the diameters of the air molecules and the tiny aerosols in the Earth's atmosphere, so it is impossible to estimate the colors of an outdoor scene precisely by using the Rayleigh scattering law of light. In 2002, Thompson derived a spatial post-processing algorithm of night scene [5] based on the visual noise (VN) and the loss of acuity (LA). There are four strategies in Thompson algorithm: (A) color space transform (CST), (B) day to night conversion (DNC), (C) night filter (NF), and (D) Gaussian noise generator (GNG). It can generate more realistic night scene, but it neglects the time factor so it cannot clearly illustrate the differences between early night, middle night and midnight. Alexander Toet used the method introduced by Welsh et al to transfer a source image's color characteristics to a grayscale target image (night vision imagery)[6,7]. They search a color source image that resembles the target scenes first. Second, they transformed both the source image and the target image into a perceptually miscorrelated color space. Third, they searched for the best matching source pixel for each target pixel from the source image by using the first order statistics of the luminance distribution in a 7×7 window around the source and target pixels. Finally, they assigned the matching pixel's chromaticity values of the source image to the target pixel. Although they effectively give single-band intensified night vision gray imagery a full color day-time image, but to find a suitable resembled color source image for the target image is not easy, and the final colors of the chromatic target image completely depends on the colors of the source image. They are not the true colors of the target image taken in day. Other papers about the scenes can be found in [8-19]

The multiple regression is a related statistical method, it is used to model the relationships between several independent variables and a dependent variable by fitting an equation to observed data. Numerous experiments have shown that the multiple regression models can be used to make accurate predictions. Multiple regression procedures are very widely used in the social and natural sciences today[20-22]. It might be a good and suitable method for us to simulate the time scene.

The red, green and blue are the primary components of light (or color image) in spatial domain. It is reasonable to take the multiple regression on each component individually. But, the spatial pixels of an image are often correlative, so the spatial domain of an image is not suitable for taking multiple regression. The DCT has properties of noise filtering, miscorrelation, and feature preservation. It is often used as a preprocessing step followed by a sophisticated algorithm in image processions, and it always has good performance while one combines the DCT block transformation with other techniques. In some cases, it has been showing that the processing based on DCT has significantly better results than the directive pixel based processing [23,24]**.** To take time scene simulation on the DCT domain by using multiple regression will be a good idea. The remainder of this paper is organized as follows: Section 2 presents the the time scenes simulation algorithm (TSSA). Empirical results is described in the Section 3. Finally, Section 4 concludes this paper.

2. The Algorithm of Time Scenes Simulation (TSSA)

2.1 The construction of the multiple regression functions database

The basic understanding of color perception of the human visual system shows the fact, which human eyes pick out the color of an object illuminated by white light is the reflection of selected wavelengths of light by that object [25-26]. The appearance color of an object can be considered as the object absorbing all colors except the colors that are reflected. For example, a red object illuminated by white light absorbs nearly all of the wavelengths except those corresponding to red light. Although there are an unlimited number of colors just as there are immeasurable quantities of real numbers on a number line, colors of the range of human visual sensations can be produced by the mixtures of finite visual lights of various wavelengths. Human eyes have three cones shaped light detectors [27]. Each cone is sensitive to a special range of colors. One is sensitive to primarily red, a second to primarily green, and a third to primarily blue. The three sensitivity ranges overlap in fact. Each cone transmits a nerve pulse to the brain at a rate proportional to the light's intensity of that cone detects. By combining the signal rates transmitted from three cones, the brain attempts to conclude what color and brightness of the light must be. Thus, to combine various quantities of three colors (red, green and blue) of light can turn out all colors that can be perceived for human.

In televisions, computer monitors, and colored image projection systems, only the three colors are enough to adequately represent any of the unlimited visible colors [28]. For measuring or reproducing color, a number of three dimensional color models have been defined; Color models like as HIS, L*a*b*, YIQ, YUV, and YCbCr are suitable for image processing applications, they are the reducing redundancy models of the image in RGB color space, obtained by some color transform from RGB color space, They are suitable for image processing applications, but not suitable for the color representation of a color image. The image in RGB color space is not suitable for image processing applications, because the image in RGB color space is highly correlated, but it is the most suitable for the color representation of a color image. Most imaging devices (CCD cameras, CRT monitors, etc) mimic the retina and utilize three separate channels calibrated for the detection of red, green and blue phosphors to render colors at every pixel on the screen [29]. The RGB color model is the most popular and natural color model. Due to it can compose any color adequately; it is frequently used in color image representation. R, G and B component of a color are given by:

$$R,G,B = k\int_{400}^{700} I(\lambda)\Phi(\lambda)S_{R,G,B}(\lambda)d\lambda \quad (3)$$

where k is a constant that defines the total overall brightness response of the human eyes, $I[\lambda]$ is the illumination spectral intensity of a color, $\Phi[\lambda]$ is the object spectral reflectivity, $S_{R,G,B}[\lambda]$ is the spectral sensitivity of the R or G or B channel of the detector and λ is the wavelength. The normalized red, green, and blue coordinates are defined as follow:

$$r = R/(R+G+B) \quad (4)$$

$$g = G/(R+G+B) \quad (5)$$

$$b = B/(R+G+B) \quad (6)$$

where R, G and B are the intensities of red, green, and blue light at a given pixel [30]. We demonstrated that color images could be represented using three primary colors.

In order to obtain the more accuracy regression of a scene image, the original image is first spilt into its R, G, and B components. Its final simulation image is reconstructed by composing these regression color components.

2.2 The construction of the multiple regression functions database

When performing experiment, we frequently tabulate data in the form of ordered pairs $(x_1, y_1), (x_2, y_2), ..., (x_n, y_n)$ with each x_i distinct. Given the data, it is then usually desirable to be able to predict y from x by finding a mathematical model, that is, a function $y = f(x)$ that fits the data as closely as possible. One way to determine how well the function $y = f(x)$ fits these order pairs $(x_1, y_1), (x_2, y_2), ..., (x_n, y_n)$ is to measure the sum of squares of the errors (SSE) between the predicted values of y and the observed values y_i for all of the n data points. Multiple linear regression is one of the widely used statistical techniques [20-22]. This technique is used to find a polynomial function of degree k, $y = \beta_0 + \beta_1 x + \beta_2 x^2 + ... + \beta_k x^k$ as the predicting function, that has the minimum of the sum of squares of the errors(SSE) between the predicted values of y and the observed values y_i for all of the n data points $(x_1, y_1), (x_2, y_2), ..., (x_n, y_n)$.

This paper proposed a way to construct the sunset scene of a scene image taken at anytime by TSSA. Fig.3 is the flow chart of the construction of the multiple regression functions database. At the beginning of the process, the R, G, and B planes of the decomposed color input image were split into non- overlapping 8 × 8 blocks, and then transferred into the frequency domain from the spatial domain by block DCT respectively. In the DCT domain, most of the signal information tends to be concentrated in a few low-frequency components. And the DC coefficient carry information about average luminance within the DCT blocks, the DC coefficient becomes the most meaningful when considering how the luminance is changing between the images [23, 24]. We took the average of the DC components of all the 8 × 8 DCT blocks to serve as the average value of the reflective color at that time. Then, we used multiple regression to find multiple regression functions of the DCT coefficients of these color-block images that were regularly photographed by fixed time interval from 17:00 to 19:30 of a day. These multiple regression functions were then constructed into a table as the database. Fig.4 shows the image of a color- block taken at 17:20, its R, G, B component images, and the images of DCT coefficients of the R, G, B component images. Table 1-3 are the tables of the average magnitudes of the 8 × 8 DCT coefficients for the R, G, B component images of the color-block. There are 64 bases for each table, the upper left base is the block's mean and it is also called the DC value of the image, another 63 bases are called the AC values of the image. Table 1-3 show that the DC value is much larger than the AC values. And the higher frequencies AC values are lesser. Fig.5, Fig.6, and Fig.7 show parts of the curves of the best fitting functions for color-block s' DC components with respect to time. Table 4 is the table of the best fitting functions' coefficients of the color-block image in DCT domain.

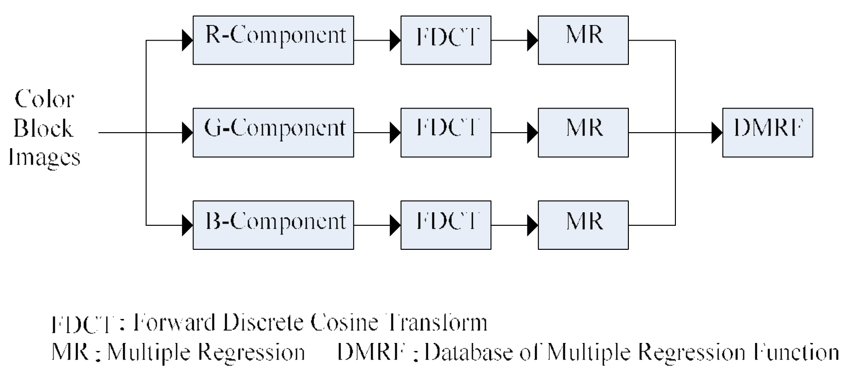

Fig. 3 The construction of the multiple regression functions database

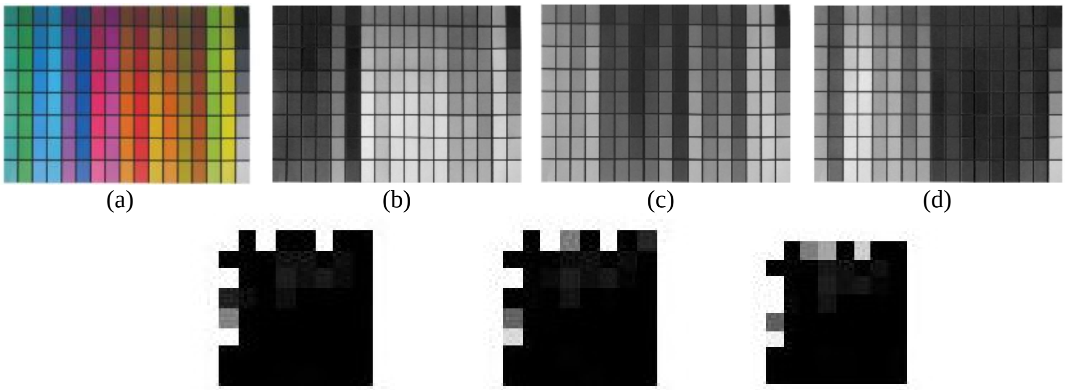

Fig. 4 The image of a color- block taken at 17:20(a) real image (b) R component image(c) G component image (d) B component image(e)The image of DCT coefficients of the R component(f)The image of DCT coefficients of the G component (g)The image of DCT coefficients of the B component.

Table 1 The DCT coefficients for the R component of the color-block image in Fig.4.

945.6788	-3.11356	2.458706	-0.33716	-1.17563	1.24538	-0.23217	-0.927
-5.97103	-0.1986	-0.02393	0.069363	0.06657	-0.00409	0.057666	-0.00114
16.23694	-0.16898	-0.09017	0.10713	0.059559	0.099738	0.041851	-0.04458
0.121902	0.048323	-0.05908	0.059259	-0.03403	0.005014	0.003166	-0.01487
0.504839	-0.04899	0.000112	-0.01591	-0.01855	0.003226	-0.00636	0.00413
1.000081	-0.02425	0.00065	-0.01323	0.0005	-0.00932	0.000607	0.003872
-0.23579	-0.00222	-0.02985	-0.00037	0.003775	0.001865	0.000458	0.003585
-0.48485	-0.01236	-0.00196	0.004875	0.008721	-0.0107	-0.00418	0.006822

Table 2 The DCT coefficients for the G component of the color-block image in Fig.4.

857.0752	-1.16039	2.932919	0.480016	-1.19657	1.780491	-0.24423	0.147122
-5.24403	-0.09254	-0.00674	0.0505	0.059852	-0.00823	0.049707	-0.01809
13.04633	-0.1286	0.039403	0.10974	0.055904	0.090136	0.021017	-0.02801
-0.13035	0.011812	-0.05759	0.071962	-0.03963	0.006384	0.003408	-0.01158
0.38559	-0.03216	0.005886	-0.01135	-0.01836	0.004468	0.000146	0.00476
0.849799	-0.02725	-0.00554	-0.01184	-0.00021	-0.01611	-0.00312	-0.00392
-0.27928	-0.01216	-0.03458	0.009935	0.002494	-0.01045	0.006994	-0.00207
-0.51225	-0.00888	-0.00602	-0.0013	0.007954	-0.00337	0.001674	0.006048

Table 3 The DCT coefficients for the B component of the color-block image in Fig.4.

756.0942	-1.61977	0.49209	0.649581	-1.17632	0.806817	-0.05249	-1.09367
-9.92855	-0.18361	-0.04784	0.088409	0.064015	0.004417	0.064835	-0.0194
7.803619	-0.11323	-0.01613	0.111271	0.064356	0.089781	0.027291	-0.05435
2.570166	0.024903	-0.05725	0.078386	-0.03275	-0.00292	0.0057	-0.01229
0.369813	-0.0401	-0.00135	0.000356	-0.01725	0.002273	-0.00308	0.003574
0.945137	-0.02902	-0.00551	-0.00782	0.000382	-0.0164	0.000275	-6.6E-05
-0.23514	-0.01996	-0.03039	0.009302	0.005829	-0.00298	0.00189	0.010154
-0.48137	-0.01432	-0.00211	0.005969	0.005762	-0.00335	-0.00572	0.005044

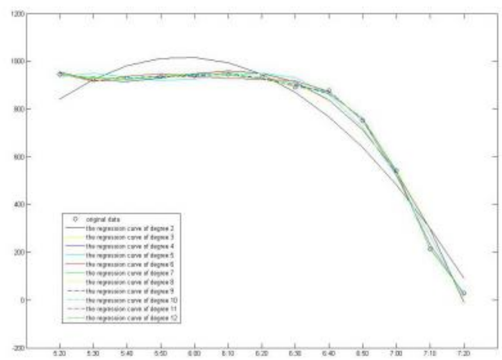

Fig. 5 Multiple regression curves of red component: the blue circle curve denotes the original data.

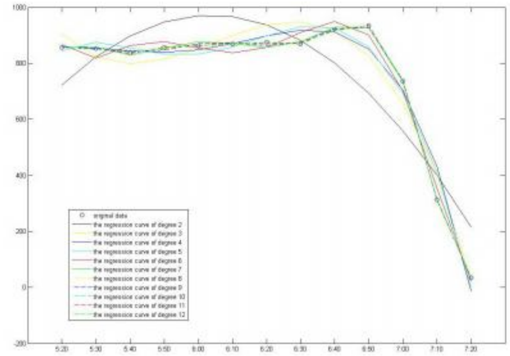

Fig. 6 Multiple regression curves of green component: the blue circle curve denotes the original data.

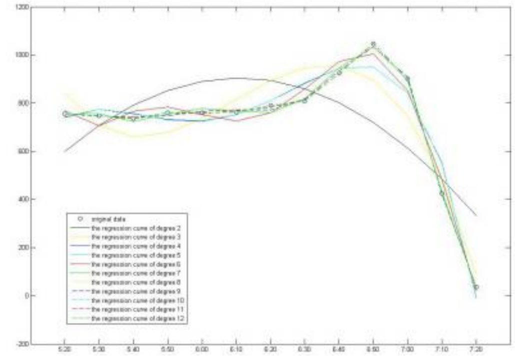

Fig. 7 Multiple regression curves of blue component: the blue circle curve denotes the original data.

Table 4 The table of the best fitting functions' coefficients of the color-block image's in DCT domain(a) R component (b) G component (c) B component.

(a)

	β_{12}	β_{11}	β_{10}	β_{9}	β_{8}	β_{7}	β_{6}	β_{5}	β_{4}	β_{3}	β_{2}	β_{1}	β_{0}
Order2											-13.2962	123.7742	730.6274
Order3										-1.63488	21.03639	-75.6819	1005.288
Order4									0.039167	-2.73158	31.16965	-110.071	1037.249
Order5								0.053630	-1.83788	21.1338	-102.101	199.7426	818.4382
Order6							0.01931	-0.75742	11.31100	-82.0910	299.9474	-505.799	1226.703
Order7						0.003697	-0.16186	2.816413	-24.9947	119.474	-297.114	339.2380	805.7708
Order8					0.00033	-0.014656	0.264853	-2.51533	13.71579	-45.3054	96.80501	-132.120	1014.710
Order9				-8.25E-05	0.00553	-0.153997	2.334163	-21.1463	118.1645	-405.519	822.4690	-891.758	1321.280
Order10			3.9E-05	-0.002816	0.088438	-1.581904	17.71574	-128.719	608.8655	-1832.91	3325.157	-3241.73	2198.855
Order11		8.19E-05	-0.0062	0.210974	-4.10367	51.07476	-425.105	2401.32	-9146.71	22841.61	-35256.63	29861.09	-9377.09
Order12	4.3E-05	-0.00351	0.12828	-2.750093	38.43666	-367.8676	2463.576	-11584.4	37773.84	-82779.6	114789.6	-89424.7	30039.45

(b)

	β_{12}	β_{11}	β_{10}	β_{9}	β_{8}	β_{7}	β_{6}	β_{5}	β_{4}	β_{3}	β_{2}	β_{1}	β_{0}
Order2											-13.0156	139.9415	595.395
Order3										-2.76017	44.9481	-196.799	1059.11
Order4									-0.27396	4.91089	-25.9311	43.7429	835.548
Order5								0.036045	-1.53556	20.95117	-115.504	251.973	688.482
Order6							0.031273	-1.27746	19.75916	-146.222	535.6168	-890.658	1349.67
Order7						0.009288	-0.42387	7.700569	-71.4466	360.1421	-964.295	1232.207	292.223
Order8					0.00061	-0.02509	0.375602	-2.28865	1.079074	51.42051	-226.272	349.1007	683.678
Order9				-0.00012	0.00786	-0.21924	3.258884	-28.2482	146.6131	-450.484	784.834	-709.344	1110.84
Order10			-0.00014	0.00942	-0.28119	4.759176	-50.3693	346.8082	-1564.22	4526.160	-7940.83	7483.901	-1948.84
Order11		1.5E-05	-0.00129	0.04866	-1.05071	14.42496	-131.654	811.2297	-3354.99	9055.481	-15023.1	13560.34	-4073.75
Order12	2.7E-05	-0.00225	0.08349	-1.81711	25.75388	-249.5500	1688.499	-8001.19	26209.5	-57496.3	79520.94	-61601.5	20762.6

(c)

	β_{12}	β_{11}	β_{10}	β_9	β_8	β_7	β_6	β_5	β_4	β_3	β_2	β_1	β_0
Order2											-11.8791	144.1064	466.4746
Order3										-3.66229	65.02901	-302.693	1081.739
Order4									-0.58273	12.65442	-85.7341	208.9524	606.2239
Order5								0.002629	-0.67476	13.82439	-92.2675	224.1406	595.4969
Order6							0.03819	-1.60144	25.3306	-190.331	702.8918	-1171.26	1402.950
Order7						0.011840	-0.54201	9.843179	-90.9326	455.151	-1209.11	1534.836	54.98319
Order8					0.00127	-0.05930	1.11207	-10.8239	59.1185	-183.575	317.8226	-292.258	864.8813
Order9				-9.6E-05	0.00737	-0.22279	3.540052	-32.6842	181.671	-606.224	1169.265	-1183.56	1224.589
Order10			-0.00023	0.015857	-0.47647	8.110404	-86.2262	595.1088	-2682.03	7723.994	-13436.3	12530.81	-3896.89
Order11		-7.8E-06	0.00037	-0.00445	-0.07813	3.106907	-44.1489	354.7011	-1755.05	5379.392	-9770.22	9385.333	-2796.94
Order12	3.5E-05	-0.00294	0.110401	-2.42578	34.70793	-339.4705	2317.982	-11081.74	36612.81	-80989.2	112925.6	-88157.1	29434.75

2.3 The simulation image synthesis of time scene

Fig. 8 is the flowchart of the simulation image of time scene. To synthesize the scenes at specific time from the scene taken at any daytime, the input image was divided into R, G, and B planes firstly. The R, G, and B components of a scene photographed at time t_1 are processed respectively with the same steps; they were transferred to the frequency domain by forward discrete cosine transform (FDCT) firstly. Then compared the DC component with the DC component of color-block at time t_1 to find the compensated coefficient c_1, to find the corresponding DC component $f_{i,j}(t_2)$ at time t_2 from looking up the database table, and then to combine $f_{i,j}(t_2)$ and c_1 to determine the final R, G, B components $g_{i,j}(t_2)$ of the simulation scene at time t_2 on frequency domain. Finally, we took the inverse discrete cosine transform (IDCT) on $g_{i,j}(t_2)$, and combined them to form the color simulation image at time t_2 of the scene.

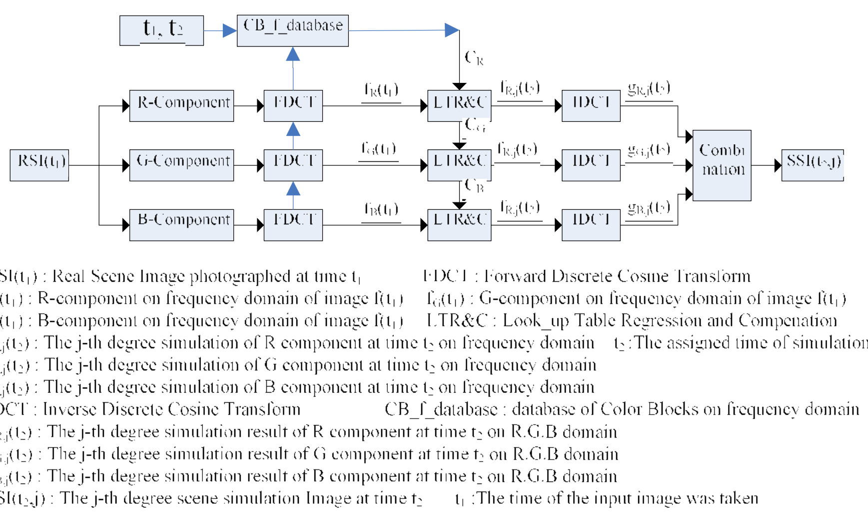

Fig. 8 The flow chart of the simulation image synthesis of a time scene.

3. Empirical results

Several test images with size (720 × 512) were used in simulation for demonstrating the performance of the proposed scheme. In order to give a detailed description of the simulation results, Fig. 9 is used to express the simulation results; comparing the corresponding simulation image with the real image, we found some lamplights in the real image taken at 19:00, but not in the corresponding synthesis image. Apart from the lamplights, the human eyes can not feel any difference between them. Table 5 shows the absolute error ratios of simulation image with respect to the real image of Fig.7. From the error table we can find that the error in R plane is the largest and the error in B plane is the smallest, this is caused by the fact that the average pixel value in B plane is larger than the average pixel value in R plane. On the other hand, the error in order 2 and order 3 best fitting regressions are much larger than the error in order larger than 3 best fitting regressions. This coincides with the Rayleigh scattering theory of sunlight. Experimental results show that there is no difference in visual quality between the simulation image obtained by our algorithm and the real image. However, because our algorithm is carried out in the DCT domain, it is time-saving and simpler.

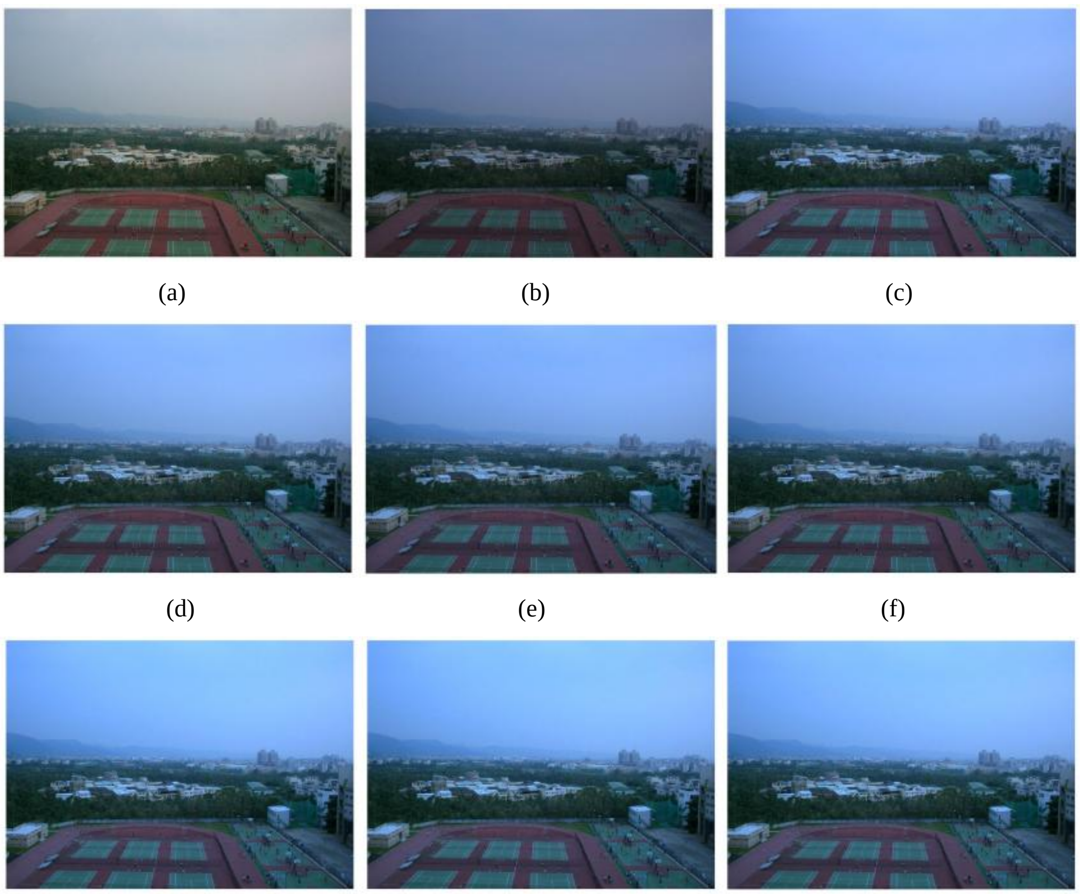

(a) (b) (c)

(d) (e) (f)

(g) (h) (i)

(j) (k) (l)

Fig. 9 Test images, (a) a scene photographed at 17:30 PM, (b)~(k) degree 2~degree 11 simulation scene at 19:00, (l) a scene photographed at 19:00 PM.

Table 5 Table of absolute error ratios of simulation image with respect to real image of Fig. 9.

	Order2	Order3	Order4	Order5	Order6	Order7	Order8	Order9	Order10	Order11	Order12
Error in R plane(%)	21.2783	13.836	13.9063	15.107	14.967	13.993	13.9398	14.0491	14.029	13.9107	13.9061
Error in G plane(%)	30.7009	10.4657	9.8452	11.5594	11.3879	8.1068	8.0967	8.1322	8.1389	8.1262	8.1262
Error in B plane(%)	34.5141	9.8316	9.9786	9.9983	10.0248	10.0654	10.0527	10.0286	10.042	10.0334	10.0329
Complexity	n^2	n^3	n^4	n^5	n^6	n^7	n^8	n^9	n^{10}	n^{11}	n^{12}

4. Conclusion

For any degree of best fitting simulation using a computer with Intel Pentium D 280GHz CPU and 512MB RAM, it only takes 3 seconds to simulate a scene image of size 720 × 512 by our look-up table algorithm. On the other hand, simulating the same image by regression simulation with the same computer takes more than 540 seconds. Table 1 is the table of absolute error ratios of simulation with respect to real image. It shows that the absolute error ratio of each degree simulations are always less than 16%; this error ratio can not be found by human eyes and it can be reduced by adopting more frequency bands in DCT domain of images for regression and simulation. However, adopting more frequency bands is going to take more time and need more computer memory. With the above experimental results and performance analyses, we conclude that the proposed approach has three major advantages: (A) Using the color-block images instead of using the scene images of a place to create the reference database, this approach is suitable for any outdoor scene taken at anywhere at anytime. (B) Taking the multiple regression on the DCT coefficients of scene images instead of taking the multiple regression on the spatial pixels of scene images, this approach simplifies the regression procedure and saves the processing time. (C) Using look-up table algorithm to save time. With this algorithm, one can successfully and effectively simulate the anytime scene from a outdoor scene taken at anytime no matter it is of uniform color or complex colors, so it is very suitable to be used in the design of virtual reality and the recognition of natural scenes.

References

[1] Van de Hulst HC., “Light Scattering by small particles,” Dover Publications, New York, 1981

[2] Maarten Sneep and Wim Ubachs, “Direct measurement of the Rayleigh scattering cross section in various gases,” Journal of Quantitative Spectroscopy & Radiative Transfer, Vol. 92, pp. 293 - 310, 2005.

[3] R. V. Deelen, J. Landgraf and I. Aben,

"Multiple elastic light scattering in the Earth's atmosphere: a doubling- adding method to include rotational Raman scattering by air," Journal of Quantitative Spectroscopy & Radiative Transfer, Vol. 95, pp. 309- 330, 2005.
[4] S. M. Lea and J. R. Burke, "Physics: The nature of things", annotated instructor's edition 1997, West company, USA, pp. 597-626.
[5] W. B. Thompson, P. Shirley, and J. A. Ferwer, "A Spatial Post- Processing Algorithm for Images of Night Scenes," Journal of Graphics Tools, Vol. 7, No. 1, pp. 1- 12, 2003.
[6] T. Welsh, M. Ashikhmin, K. Mueller, Transferring color to greyscale images. Proceedings of 29th annual conference on computer graphics and interactive techniques, ACM Press, New York, USA, 2002, pp. 277–280.
[7] Alexander Toet ,'Colorizing single band intensified nightvision images', Displays, Vol. 26, No. 1, pp: 15-21, 2005
[8] Arthur R. Weeks, Jr., "Funamentals of Elecroni Image Processng", SPIE/IEEE Series on Image Science & Engineering, Bellingham, Washington USA, pp. 440-451, 1998.
[9] Angus M. Brown, "A step-by-step guide to non-linear regression analysis of experimental data using a Microsoft Excel spread sheet", Computer methods and programs in Biomedicine 65, pp. 191-200, 2001.
[10] C. J. Vianna, E. A. De Souza, Combining Marr and Canny Operators to Detect Edges, Microwave and Optoelectronics Conference, 2003. Vol. 2, pp. 695-699.
[11] E. Bourennane, P. Gouton, M. Paindavoine, F. Truchetet, Generalization of Canny- Deriche filter for detection of noisy exponential edge, Signal processing 82 (2002) 1317- 1328.
[12] G. Qiu and J. Duan, "An Optimal Tone Reproduction Curve Operator for the Display of High Dynamic Range Images," IEEE International Symposium on Circuits and Systems, pp.6276-6279, 2005.
[13] G. W. Larson, H. Rushmeier, and C. Piatko, "A Visibility Matching Tone Reproduction Operator for High Dynamic Range Scenes, "IEEE Trans. On Visualization and Computer Graphics, Vol. 3, No. 4, pp.291-236, 1997.
[14] H. Zhang and L. Lucchese, "A Fast Tone Reproduction Algorithm for High Dynamic Range Image Display," 2004 IEEE 6th Workshop on Multimedia Signal processing, pp. 275-278. 2004.
[15] J. A. Ferwerda, "Elements of Early Vision for Computer Graphics," IEEE Computer Graphics and Applications, Vol. 21, No.5, pp. 22-33, 2001.
[16] J. Tumblin and H. Rushmeler, "Tone Reproduction for Realistic Images, IEEE Computer Graphics and Applications, Vol. 13, No.6, pp. 42-48, 1993.
[17] M. Boutell and J. Luo, "Sunset Scene Classification Using Simulated Image Recomposition," Proceeding, IEEE Int'l Conf. on Multimedia and Expo, pp.I.37-I.40, 2003.
[18] M. Hermon, "Generating Detailed Scene Descriptions, "IEEE Int'l Conf. On Robotics and Automation, Vol. 2, pp.426-431, 1986.
[19] R. C. Gonzalez and R. E. Woods, "Digital image processing," 2nd ed., New Jersey: Prentice-Hall, 2002, pp. 675-683.
[20] C. C. Liu and W. Y. Chen, " Screw pitch pression measurement using simple linear regression and image analysis", Applied Mathematics and Computation, Vol. 178, pp.390- 404, 2006.
[21] J. S. Milton, J. C. Arnold, "Introduction to probability and statistics",4th edition 2003, McGraw-Hill companies, New York, pp. 448-457
[22] S.I.V. Sousa, F.G. Martins, M.C.M. Alvim-Ferraz, M.C. Pereira, "Multiple linear regression and artificial neural networks based on principal components to predict ozone concentrations", Environmental Modelling and Software, Vol. 22, No. 1, pp. 97-103, 2007
[23] Daidi Zhong , Irek Defée, "DCT histogram optimization for image database retrieval", Pattern Recognition Letters, Vol. 26, No. 14, pp. 2272-2281, 2005
[24] J. Tang, " A contrast based image fusion technique in the DCT domain", Digital Signal Processing, Vol. 14,p.218-226, 2004
[25] S. S. Deeb, "Genetics of variation in human color vision and the retinal cone mosaic", Current Opinion in Genetics & Development, Vol: 16 ,No.3, pp. 301-307, 2006
[26] Lennie, Peter, "Color vision: Putting it

together", Current Biology, Vol. 10, No.16, pp. R589-R591, 2000
[27] S. D.Buluswar, B. A. Draper, "Color Models for Outdoor Machine Vision," Computer Vision and Image Understanding, Vol.85, No.2, pp. 71-99 , 2002
[28] C. Clausen and H. Wechsler, "Color Image Compression Using PCA and Backpropagation Learning, " pattern recognition, Vol. 33, pp1555-1560, 2000
[29] T. Bose, "Digital signal and image processing", 2004, J. Wiley & sons,New York
[30] I. Andreadis and Ph. Tsalides, "Analog computation of Image Chromaticity," Real-Time Imaging 3,pp.1-6, 1997